

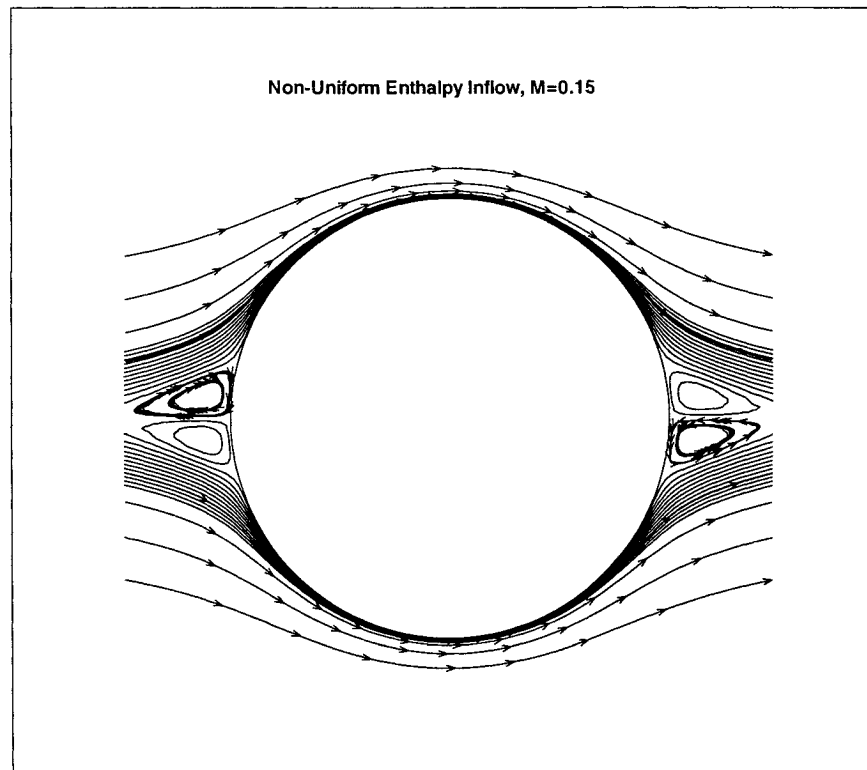


A01-31156

AIAA 01-2595

**A Third-Order Fluctuation Splitting Scheme
That Preserves Potential Flow**

Hiroaki Nishikawa and Mani Rad and Philip Roe
*W. M. Keck Foundation Laboratory for Computational Fluid Dynamics
Department of Aerospace Engineering
The University of Michigan, Ann Arbor, MI 48109*



**15th Computational Fluid Dynamics
Conference
June 11-14, 2001/Anaheim, CA**

A Third-Order Fluctuation Splitting Scheme That Preserves Potential Flow

Hiroaki Nishikawa* and Mani Rad and Philip Roe†

W. M. Keck Foundation Laboratory for Computational Fluid Dynamics

Department of Aerospace Engineering

The University of Michigan, Ann Arbor, MI 48109

Introduction

We present further developments in a program to create a novel algorithm for the Euler and (ultimately) Navier-Stokes equations. The main features of the algorithm, and of the improvements reported here, are as follows.

1. The algorithm uses an unstructured grid, and is driven by residuals evaluated on simplicial cells, with unknown quantities stored at the nodes.
2. The residuals are split into components having different physical significance before being distributed to the nodes of the cell.
3. The residual is enhanced to third-order accuracy by reconstructing nodal gradients.
4. The separation between elliptic and hyperbolic components of the residual is enforced strongly (nodewise) rather than weakly (elementwise)

These features result in extremely clean solutions with very low levels of spurious entropy. In particular, it is possible to demonstrate excellent solutions to the flow over an ellipse at incidence, thereby meeting a challenge proffered by Pulliam in.¹⁰ At the same time, as a byproduct of the decomposition, the code arrives at an authentic incompressible limit, while still retaining an accurate shock-capturing ability in transonic flow.

Not yet implemented into the Euler code, but very compatible with it, are the following

- a. Nodal movement also driven by residuals, leading to
- b. Automatic realignment of element edges with characteristic lines and shocks for hyperbolic problems,
- c. Migration of nodes into under-resolved regions

*Postdoctoral Researcher, Member AIAA.

†Professor, Fellow AIAA.

Copyright © 2001 by the American Institute of Aeronautics and Astronautics, Inc. No copyright is asserted in the United States under Title 17, U.S. Code. The U.S. Government has a royalty-free license to exercise all rights under the copyright claimed herein for Governmental Purposes. All other rights are reserved by the copyright owner.

These features have been implemented only on model problems, but for these we can demonstrate arbitrarily sharp discontinuity capturing (zero width with no interior points), and accurate elliptic solutions to incompressible flow on very coarse grids. The material on hyperbolic grid adaptation has appeared elsewhere⁹ so we focus here on newer results relating to the elliptic case.

This paper is based on the doctoral theses of the first two authors^{8,11} where more details and examples can be found.

Basic Solution Strategy

We attempt to combine the most useful features of several forms of the Euler equations. In *natural variables*, (pressure, flow direction, enthalpy and entropy) the flow can be decoupled into potential and convective parts;

$$\begin{aligned} p_s - \rho a^2 \theta_n &= 0 \\ \rho a^2 \theta_s - p_n &= 0 \\ h_s &= 0 \\ S_s &= 0 \end{aligned} \quad (1)$$

This is the unique form of the equations that produces, in the linear case, a complete decoupling into elliptic and hyperbolic subsystems.¹⁷ There is an analogy with the use of characteristic form in conventional upwind codes. The discretization is designed to meet the physics of the natural variables, but a similarity transformation is used to allow the coding to be done in terms of more convenient variables.

The actual variables used are those contained in the *parameter vector* $\mathbf{z} = \sqrt{\rho}(1, u, v, h)^T$, in terms of which the steady Euler equations can be written¹³

$$\mathbf{Cz}_x + \mathbf{Dz}_y = 0 \quad (2)$$

with

$$\mathbf{C} = \begin{bmatrix} z_2 & z_1 & 0 & 0 \\ \frac{\gamma-1}{2\gamma} z_4 & \frac{\gamma+1}{2\gamma} z_2 & -\frac{\gamma-1}{2\gamma} z_3 & \frac{\gamma-1}{2\gamma} z_1 \\ 0 & z_3 & z_2 & 0 \\ z_4 & 0 & 0 & z_2 \end{bmatrix} \quad (3)$$

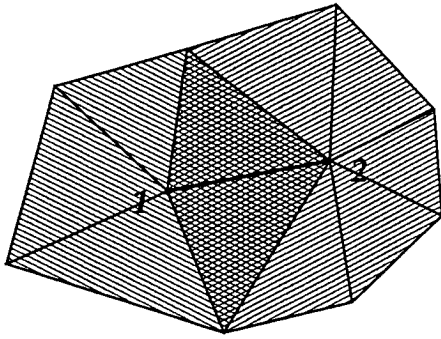


Fig. 1 Gradients at nodes A and B are obtained by applying Gauss' theorem to the shaded control volumes.

$$D = \begin{bmatrix} z_3 & z_1 & 0 & 0 \\ 0 & z_3 & z_2 & 0 \\ \frac{\gamma-1}{2\gamma} z_4 & -\frac{\gamma-1}{2\gamma} z_2 & \frac{\gamma+1}{2\gamma} z_3 & \frac{\gamma-1}{2\gamma} z_1 \\ z_4 & 0 & 0 & z_3 \end{bmatrix} \quad (4)$$

The advantage of these variables is that a simple linearization over an element with vertices 123, $\bar{z} = (z_1 + z_2 + z_3)/3$, $\bar{C} = C(\bar{z})$, $\bar{D} = D(\bar{z})$, gives a residual for that element that is conservative and hence leads to correctly captured shockwaves.³

The residual over an element E is then³

$$\phi_E = \bar{z}^T \int_{\partial E} ((\bar{C} dy - \bar{D} dx) z) \quad (5)$$

and this is *distributed* to the nodes of the element, after first being projected into the components due to the elliptic and hyperbolic parts of the flow. In previous work,⁷ this was done by analyzing the spatial gradients. The present work is based on the realization¹² that the same task can be accomplished more directly on the residual itself.

Evaluation of the integral in (5) by applying the Trapezium Rule to each side gives a second-order method. If the derivative of the integrand were available at each node then the Trapezium Rule with Endpoint Correction could be used to give a fourth-order method. One order is lost if the derivative is only an estimate. Caraeni and Fuchs² suggest to obtain these estimates as shown in Figure 1. We apply their idea in the form;

$$\int_A^B z ds = \frac{1}{2} |\Delta s| \left(z_A + z_B - \frac{1}{6} \Delta s \cdot (\nabla u_A - \nabla u_B) \right) \quad (6)$$

This correction is a little more economical than theirs. We find that it increases the cost of the calculation by only about 25% but greatly improves the accuracy.

We then define projection matrices (Π_S, Π_h, Π_p)¹² such that $\Pi_S \phi_E$ is the part of the residual due to transport of entropy, $\Pi_h \phi_E$ is the part of the residual due to transport of enthalpy, and $\Pi_p \phi_E$ is the part of the residual due to potential flow. The first two are distributed in an upwind manner using the

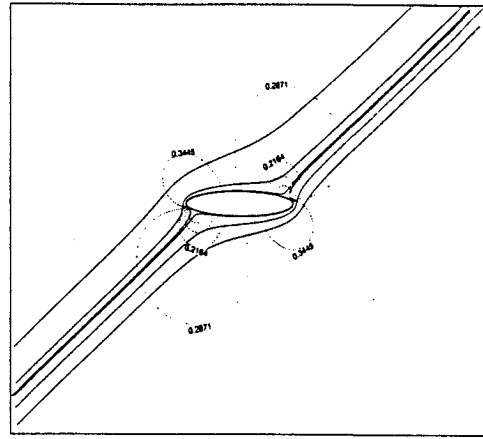


Fig. 2 Mach number profile over the elliptic body shows good symmetry.

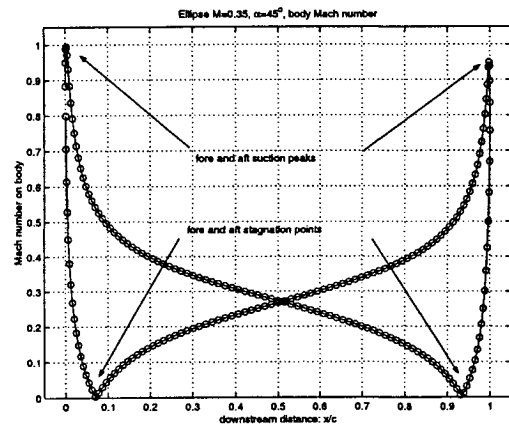


Fig. 3 The trailing edge suction peak is almost captured with same intensity as the leading-edge one.

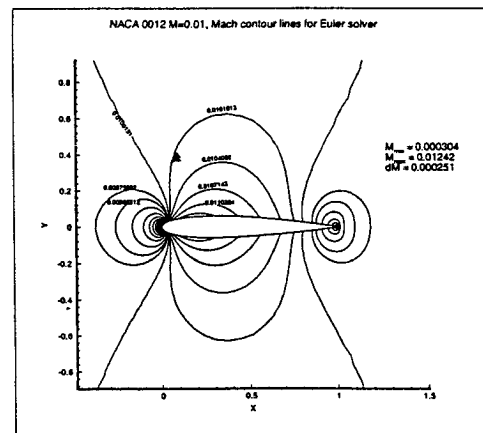


Fig. 4 NACA 0012 calculations in the incompressible regime. Mach contour plots are superimposed for comparison, showing that all solutions are self-similar in the incompressible limit.

PSI scheme⁴ in the form due to Sidilkover,¹⁸ and the third is, in subsonic flow, distributed in a least-squares fashion.

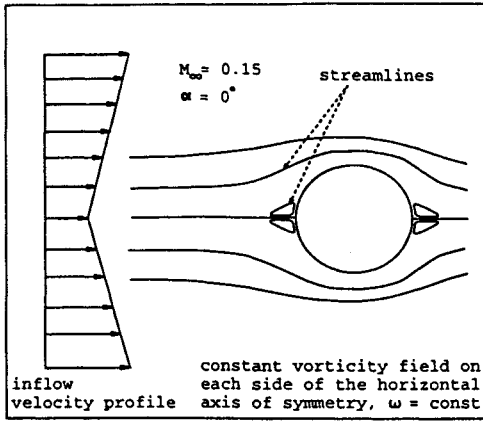


Fig. 5 Cartoon of non-uniform enthalpy inflow problem. Due to the linear inflow velocity profile, the vorticity is constant everywhere in the flow field.

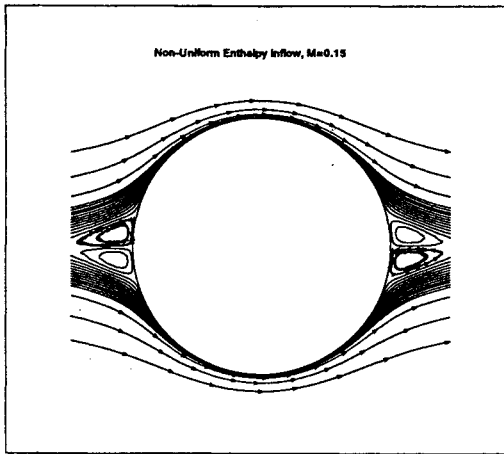


Fig. 6 Streamlines superimposed with contour lines of enthalpy (left). Since enthalpy is advected along streamlines, the two should coincide. The fore-aft symmetry of the flow is well captured as indicated by the circulation zones.

Properties and Results

For a linear problem, the above scheme has the property that the potential part of the residual does not change the entropy or enthalpy. In fact, the changes that it does create lie in the intersection of the manifolds $S = \text{const}$, $h = \text{const}$ and in the linear case this is a hyperplane. In the nonlinear case, the orientation of the corresponding hypersurface varies throughout the solution. The update vector is correctly oriented for the average state in the cell, but not quite correctly oriented for the state at any node of the cell. There are therefore small changes of entropy and enthalpy created by the potential part of the residual. These are found particularly in the vicinity of stagnation points, where the eigenstructure degenerates, but are in fact smaller by one or two orders of magnitude than those produced by usual Euler codes. However, a further improvement is possible by projecting the update at each node

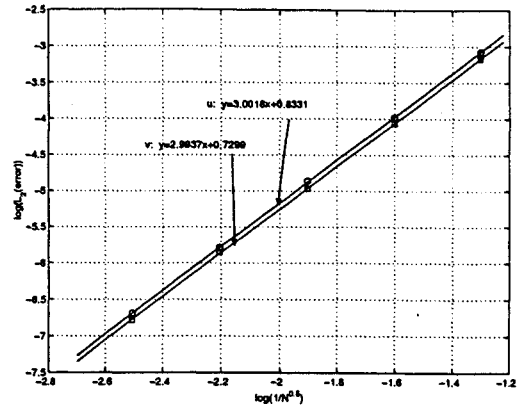


Fig. 7 Order of accuracy of the Euler solver on Fraenkel's flow shows third-order behavior.

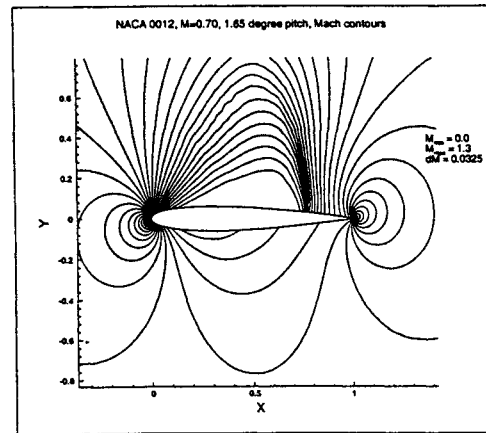


Fig. 8 NACA 0012 calculations in the supercritical regime. Mach contours for $M_\infty = 0.70$, $\alpha = 1.65^\circ$

into the hypersurface corresponding to the previous state at that node. The spurious entropy is then reduced further by three or four orders of magnitude.

The numerical dissipation is then so low that almost perfect potential flow can be recovered. In particular, the challenge proposed by Pulliam¹⁰ can be met, of computing the flow over an ellipse placed at incidence in a subsonic flow. As Pulliam observed, any orthodox Euler code will produce something like a viscous wake, with a strong fore-and-aft asymmetry and significant lift and drag. The true potential flow, of course, should give no aerodynamic forces, in accord with d'Alembert's Paradox. The results in Figures 2 and 3 show that this is rather well achieved.

A byproduct of the scheme is that it automatically incorporates preconditioning. It has been known for some time that most Euler codes, especially those based on upwind principles, give very inaccurate solutions when applied to almost incompressible flows. A theoretical explanation was given by Guillard and Viozat.⁶ An asymptotic analysis shows that pressure fluctuations in a low speed flow that is obtained analytically, scaled by the free stream sound speed

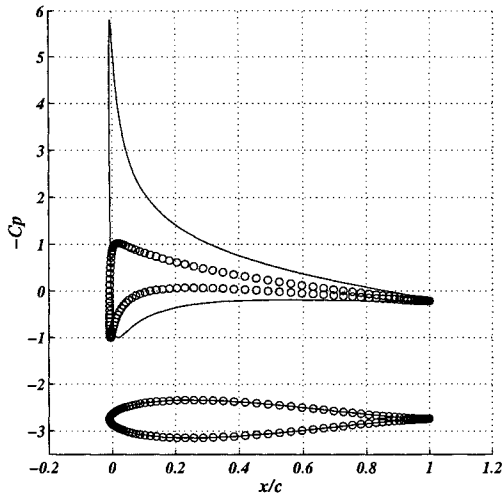


Fig. 9 C_p distribution on a Joukowski airfoil at the angle of attack 10° obtained by a least-squares scheme on a fine 160×80 regular triangular O-grid.

and density, are of order M^2 , but that those predicted by a first-order upwind scheme are of order M . Application of preconditioning^{19,20} restores the correct scaling. There is a close link between preconditioning and equation decomposition¹⁶ At the differential level, breaking the residual into its unique orthogonal components, allowing them to evolve independently, and then recombining them, recovers the preconditioner of van Leer, Lee and Roe.²⁰ The present scheme is, in effect, a direct implementation of this idea, and moreover does not suffer the slight loss of robustness near stagnation points noted by other authors. We speculate that this is due to the truly multidimensional implementation adopted here. Figure 4 shows solutions obtained for Mach numbers of 10^{-1} , 10^{-2} , and 10^{-3} superposed on one another.

The low dissipation is maintained even when the flow has variable enthalpy. Figure 5 shows the flow past a circular cylinder due to a stream that is sheared at infinity. An exact solution for this situation was given by Fraenkel.⁵ Closed regions of separated flow are found near the front and rear. The enthalpy of this flow is not uniform, but should be constant along streamlines. In Figure 6 we superpose some streamlines and some lines of constant enthalpy, showing that they coincide to within visual accuracy. In Figure 7 we demonstrate third-order grid convergence for this case.

In Figure 8 we show that our code gives a clean solution to a typical transonic problem.

Grid Movement

It was shown in¹⁴ that remarkable results for a simple hyperbolic problem could be achieved by the simple expedient of minimizing the residuals with

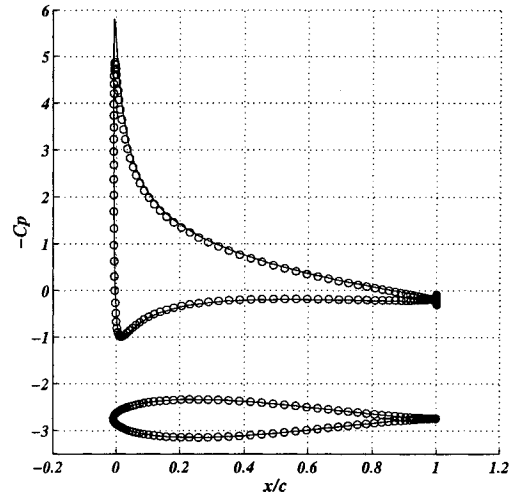


Fig. 10 C_p distribution on a Joukowski airfoil obtained by the modified least-squares scheme.

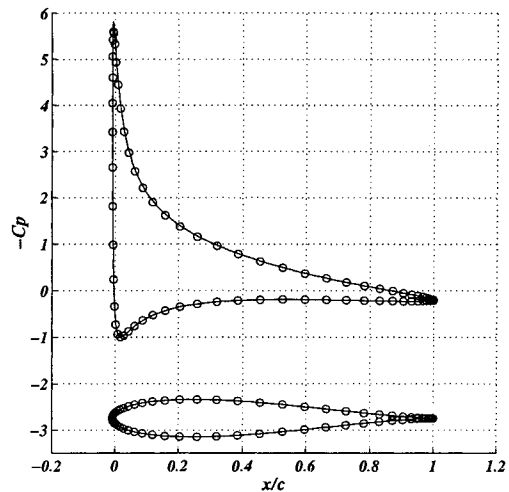


Fig. 11 A third-order solution for the airfoil problem on a 80×40 O-grid.

respect to the nodal coordinates as well as with respect to the nodal states. Both minimizations can be neatly put into the present distributive framework. It was also shown in¹⁵ that perfectly discontinuous data could be represented by allowing elements to degenerate to zero width across the characteristic direction. In⁹ the extension to nonlinear shocks was achieved, although all results obtained to date have only been for scalar model problems, or 2×2 linear systems. However in¹ results are given for the Euler equations from a scheme that requires the degenerate elements to be flagged in advance; merging of the two approaches should be fairly simple.

With good progress made on the hyperbolic case, we report here on efforts to extend the idea to the elliptic case. We have considered the Cauchy-Riemann equations

$$\delta = u_x + v_y = 0 \tag{7}$$

$$\omega = v_x - u_y = 0 \tag{8}$$

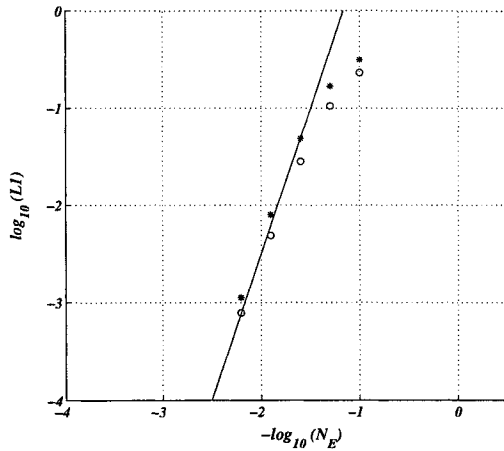


Fig. 12 The solid line indicates the line of convergence rate 3. The error in u and v were measured in L_1 norm, indicated by circles and stars respectively. N_E is the number of nodes in the radial direction of the O-grids.

as a model of incompressible flow, applied to a Joukowski airfoil for which the exact solution is known. Our first effort was to define discrete cell residuals Δ_E, Ω_E and to minimize the functional

$$\mathcal{F} = \sum_E (\Delta_E^2 + \Omega_E^2) / S_E \quad (9)$$

where S_E is the element area. This was proposed in¹⁴ and has some very attractive theoretical properties, such as reproducing, away from boundaries, the standard Galerkin method for the Laplace equations governing u and v . In fact the results were highly disappointing. Figure 9 shows the results from a “second-order” version of this method on quite a fine mesh. The problem apparently lies in correctly coupling the two Laplace equations on the boundary, through a no-flow condition. If the exact solution for either u or v was prescribed on the boundary, then a good solution for the other variable could be found. A much better solution (Figure 10, obtained on a fixed grid) was obtained with the factor S_E omitted from (9), but another disappointment was that further minimization with respect to the grid, although it necessarily reduced the residual, did little or nothing to reduce the error. From this it can be deduced that for elliptic problems there is little correlation between the error and the residual determined by a piecewise linear element. Indeed, this should not be unexpected since the error in approximating a smooth function by a piecewise linear one must depend on the local curvature, which is not accounted for in this method.

Things worked out far better after modifying the residual as in (6). On a fixed grid, we obtained the results in Figure 11. This is a better solution than we obtained with the second-order scheme using half the mesh spacing, and Figure 12 shows that third-order

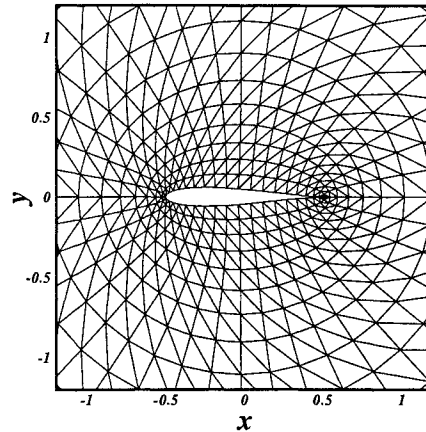


Fig. 13 Initial 40x20 O-grid around a Joukowski airfoil.

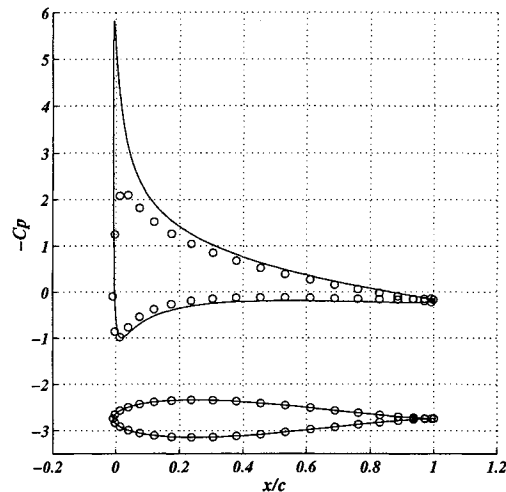


Fig. 14 C_p distribution on the initial grid.

convergence is indeed obtained. Moreover, because the residual now contains derivative information, the solution can be improved by adjusting the grid to minimize it. In Figure 13 the original grid is shown (but with the spacing again doubled) and in Figure 14 the solution on that coarse grid is shown. When the nodes are allowed to move, giving the grid in Figure 15, the much improved solution in Figure 16 is produced.

Future Work

We recognize that there is no great market for a new two-dimensional Euler solver, even a very good one. These are still preliminary studies, but encouraging in showing that clean and accurate solutions can be produced on rather coarse grids. The big benefit to be derived from this will come in three-dimensional calculations. Many of the ideas presented here do go over directly to three dimensions, but not all. The decomposition of the Euler equations in three dimensions yields two advection

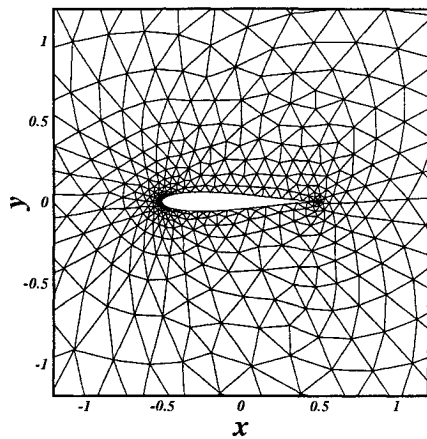


Fig. 15 Adaptive grid.

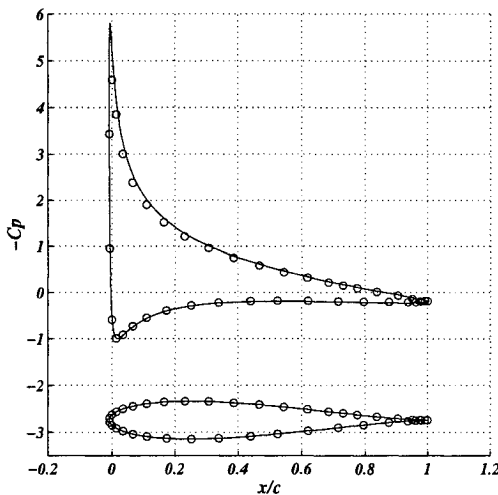


Fig. 16 C_p distribution on the adaptive grid.

equations, and a 3×3 system that does not describe potential flow, but rather Beltrami flow, in which the vorticity is always parallel to the flow direction.

This is in fact what we need in order to predict high Reynolds number lifting flows with trailing vorticity, but it leads to the numerical study of a model problem that has so far received little attention. In the supersonic case it is the wave equation written as a first-order system. In either the subsonic or supersonic cases helicity (streamwise vorticity) may exist, but does not change along streamlines. The correct numerical treatment of helicity might be a great advance toward the economical computation of strongly vortical flows. This is the next place where effort needs to be concentrated.

References

¹M. J. Baines, S. J. Leary and M. E. Hubbard, A finite-volume method for steady hyperbolic equations, in *Finite Volumes for Complex Applications II*, eds Vilsmeier, Benkhaldoun, Hanel, Duisberg, 1999, Hermes.

²D. Caraeni, L. Fuchs. A New Compact High Order Multidimensional Upwind Discretization. *Proceedings of the 4th*

World CSCC Conference, Vouliagmeni, Greece, July 10-15 2000.

³H. Deconinck, P.L. Roe, R. Struijs, A multidimensional generalisation of Roe's flux difference splitter for the Euler equations, *Computers and Fluids*, **22**, p215, 1993.

⁴H. Deconinck, R. Struijs, G. Bourgois, P.L. Roe, Compact advection schemes on unstructured grids, *Von Karman Institute Lecture Series 1993-04*, 1993.

⁵L. E. Fraenkel, On corner eddies in plane inviscid shear flow, *Journal of Fluid Mechanics*, **11**, 1961.

⁶H. Guillard, C. Viozat, On the behaviour of upwind schemes in the low Mach number limit, *Comput. Fluids* **28**, 1999.

⁷L. M. Mesaros, P. L. Roe, Multidimensional fluctuation splitting based on decomposition methods, *AIAA paper 95-1699*, 1995.

⁸H. Nishikawa, On grids and solutions from residual minimization, *Ph. D Thesis*, Aerospace Engineering, University of Michigan, 2001.

⁹H. Nishikawa, M. Rad, P. L. Roe, Grids and solutions from residual minimization, *Proc. 1st Int. Conf. on CFD*, Kyoto, 2000.

¹⁰T. Pulliam, A Computational Challenge: Euler solutions for ellipses, *AIAA paper 89-0469*, 1989.

¹¹M. Rad., A residual distribution approach to the Euler equations that preserves potential flow, *Ph. D Thesis*, Aerospace Engineering, University of Michigan, 2001.

¹²M. Rad, P. L. Roe. An Euler code that can preserve potential flow, *Finite Volumes for Complex Applications*, eds Vilsmeier, Benkhaldoun, Hanel, Duisberg, 1999, Hermes.

¹³P. L. Roe, Riemann solvers, parameter vectors, and difference schemes, *J. Comput. Phys.*, **43**, p 357, 1081.

¹⁴P. L. Roe, Compounded of many simples, reflections on the role of model problems in CFD, *Workshop on Barriers and Challenges in Computational Fluid Dynamics*, NASA Langley, August, 1996, eds Venkatakrishnan, Salas and Chakravarthy, Kluwer, 1998.

¹⁵P.L. Roe, Fluctuation splitting on optimal grids, *AIAA CFD Meeting*, Snowmass, Colorado, June 1997.

¹⁶P. L. Roe, K. Kabin, Differential preconditioning and elliptic/hyperbolic splitting of two-dimensional conservation laws, *in preparation*

¹⁷P.L. Roe, E. Turkel, The quest for diagonalization of differential systems, *Workshop on Barriers and Challenges in Computational Fluid Dynamics*, NASA Langley, August, 1996, eds Venkatakrishnan, Salas and Chakravarthy, Kluwer, 1998.

¹⁸D. Sidilkover, P.L. Roe, Unification of some advection schemes in two dimensions. *ICASE Report No. 95-10*, March 2, 1995,

¹⁹E. Turkel, V. Vatsa, R. Radespiel, Preconditioning methods for low-speed flow, *AIAA paper 96-2460*, 1996.

²⁰B. van Leer, W-T. Lee, P. L. Roe, Characteristic timestepping, or local preconditioning for the Euler equations, *AIAA paper 91-1552-CP*, 1991.